

# Characterization and thermal dehydration kinetics of zinc borates synthesized from zinc sulfate and zinc chloride

Azmi Seyhun Kipcak · Fatma Tugce Senberber ·  
Emek Moroydor Derun · Nurcan Tugrul ·  
Sabriye Piskin

Received: 15 December 2014 / Accepted: 3 February 2015 / Published online: 14 February 2015  
© Springer Science+Business Media Dordrecht 2015

**Abstract** Zinc borate hydrate ( $Zn_3B_6O_{12} \cdot 3.5H_2O$ ) was synthesized from zinc sulfate heptahydrate ( $ZnSO_4 \cdot 7H_2O$ ), anhydrous zinc chloride ( $ZnCl_2$ ), and boric acid ( $H_3BO_3$ ). The product was characterized by X-ray diffraction, Fourier-transform infrared and Raman spectroscopy, and thermal gravimetry and differential thermal gravimetry. The effects of reaction time and temperature on product morphology were studied by use of scanning electron microscopy. Results from thermal analysis showed that dehydration occurred in two steps. Thermal dehydration kinetics were investigated by use of the Coats–Redfern and Horowitz–Metzger non-isothermal kinetic methods. In the Coats–Redfern method, activation energies were found to be 225.40 and 570.63 kJ/mol for the first and second steps, respectively. In the Horowitz–Metzger method, activation energies were found to be 254.33 kJ/mol for the first step and 518.22 kJ/mol for the second step.

**Keywords** Thermal properties · Dehydration · Hydrothermal synthesis · Zinc borate

## Introduction

In nature, boron occurs in combination with metal atoms as boron minerals. Boron minerals and compounds are usually classified into two categories, hydrated and non-hydrated. So-called hydrated borates, which account for most of the boron-containing minerals and synthetic borates consumed by industry, have structures

---

A. S. Kipcak · F. T. Senberber · E. Moroydor Derun · N. Tugrul (✉) · S. Piskin  
Department of Chemical Engineering, Faculty of Chemical and Metallurgical Engineering, Yildiz Technical University, Davutpasa Campus, Davutpasa Street No. 127, 34210 Esenler, Istanbul, Turkey  
e-mail: ntugrul@yildiz.edu.tr

containing B–OH groups (hydroxy hydrated borates) and may also contain water of crystallization. Many types of borate resemble minerals in structure, containing isolated polyborate anions or complex polyborate rings, chains, sheets, or networks [1].

Zinc borates are the most important class of boron compound, because of their high fire resistance and lack of toxicity. For this reason, they are used in the plastics and rubber industries, in particular. They are also used as char promoters, anti-arcing agents, for preservation of wood composites, as modifiers of electro-optical properties, and as after-glow-suppressant additives [2–4]. Several types of zinc borate are known, for example  $2\text{ZnO}\cdot 2\text{B}_2\text{O}_3\cdot 3\text{H}_2\text{O}$ ,  $2\text{ZnO}\cdot 3\text{B}_2\text{O}_3$ ,  $\text{Zn}_2\text{B}_6\text{O}_{11}\cdot 3\text{H}_2\text{O}$ ,  $\text{Zn}_2\text{B}_6\text{O}_{11}\cdot 7\text{H}_2\text{O}$ , and  $\text{Zn}_3\text{B}_{10}\text{O}_{18}\cdot 14\text{H}_2\text{O}$ ; of these, the most important commercially is  $3\text{ZnO}\cdot 2\text{B}_2\text{O}_3\cdot 3.5\text{H}_2\text{O}$  [5–7].

Ting et al. [8], prepared nano-zinc borates from zinc nitrate ( $\text{Zn}(\text{NO}_3)_2\cdot 6\text{H}_2\text{O}$ ), borax ( $\text{Na}_2\text{B}_4\text{O}_7\cdot 10\text{H}_2\text{O}$ ), and ammonia ( $\text{NH}_3$ ); reaction times were between 6 and 15 h at 45 °C. Zheng et al. [9] synthesized zinc borate in the form  $4\text{ZnO}\cdot \text{B}_2\text{O}_3\cdot \text{H}_2\text{O}$  by addition of  $\text{Zn}(\text{NO}_3)_2\cdot 6\text{H}_2\text{O}$  to a mixture of  $\text{Na}_2\text{B}_4\text{O}_7\cdot 10\text{H}_2\text{O}$  and a phosphate ester and heating at 70 °C for 7 h.  $\text{Zn}_2\text{B}_6\text{O}_{11}\cdot 7\text{H}_2\text{O}$  and  $\text{Zn}_3\text{B}_{10}\text{O}_{18}\cdot 14\text{H}_2\text{O}$  have been prepared from  $\text{Na}_2\text{B}_4\text{O}_7\cdot 10\text{H}_2\text{O}$  and a mixture of zinc oxide (ZnO) and  $\text{ZnSO}_4\cdot 7\text{H}_2\text{O}$ , by boiling for 11 h [6]. Tugrul et al. [10], prepared hydrophobic nanostructured zinc borate by reaction of zinc borate hydrate modified with oleic acid at 95 °C.

Thermal decomposition of metal borates usually involves dehydration, as a result of removal of water of crystallization from the structure. The characteristic features of dehydration of materials should be known to enable design of equipment and to reduce the mass of materials required, thus reducing transportation costs. The thermal dehydration behavior of boron minerals may be studied by different methods, for example supercritical drying.  $\text{ZnO}\cdot \text{B}_2\text{O}_3\cdot 2\text{H}_2\text{O}$  decomposes to ZnO and  $\text{H}_3\text{BO}_3$  on supercritical ethanol drying at 250 °C and 6.5 MPa. In supercritical carbon dioxide drying of methanol–zinc borate mixtures, zinc borate was obtained from ZnO and  $\text{H}_3\text{BO}_3$  and there was no chemical interaction with  $\text{CO}_2$ . Carbonates were formed on the surface of zinc borate obtained from borax decahydrate and zinc nitrate hexahydrate [11–14]. Although structural details are known for the most commercially relevant crystalline hydrated borates, the thermal dehydration kinetics of several important zinc borates have not been described.

According to the literature, combinations of  $\text{ZnSO}_4\cdot 7\text{H}_2\text{O}$  and  $\text{ZnCl}_2$  with NaOH and  $\text{H}_3\text{BO}_3$  have not been used as starting material for synthesis of zinc borates. Long reaction times (6–15 h) are reported for synthesis of zinc borates. Also, because the thermal dehydration kinetics and effects of reaction temperature on the morphology of zinc borates have not been studied, in the work discussed in this paper we synthesized zinc borates from these raw materials and attempted to reduce reaction times, with the objective of saving energy. The pure zinc borate compounds synthesized were characterized by X-ray diffraction (XRD), Fourier-transform infrared (FT-IR) spectroscopy, Raman spectroscopy, scanning electron microscopy (SEM), and thermal gravimetry–differential thermal gravimetry (TG/DTG).

## Experimental

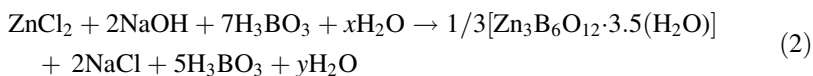
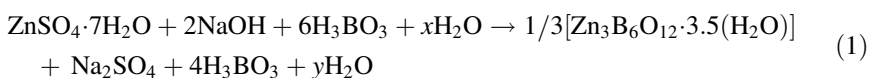
### Preparation and characterization of the raw materials

The zinc sources  $\text{ZnSO}_4 \cdot 7\text{H}_2\text{O}$  and  $\text{ZnCl}_2$  were obtained from Sigma Aldrich; the purity was Reagent Plus<sup>®</sup> ( $\geq 99.0\%$  purity) and reagent grade ( $\geq 98.0\%$  purity), respectively. The boron source  $\text{H}_3\text{BO}_3$  was obtained from Bandirma Boron Works; the minimum purity was  $99.9\%$ .  $\text{H}_3\text{BO}_3$  was pretreated by grinding and sieving to furnish a particle size  $< 75\ \mu\text{m}$ . NaOH of minimum purity of  $98\%$  was obtained from Merck Chemicals. XRD analysis was performed with a Philips PANalytical Xpert Pro (step:  $0.030^\circ$ , time for step:  $0.50\ \text{s}$ , scan speed:  $0.060\ ^\circ/\text{s}$ , range  $7^\circ\text{--}90^\circ$ ) at  $45\ \text{kV}$  and  $40\ \text{mA}$ , using X-rays produced in a Cu-K $\alpha$  tube.

### Zinc borate synthesis

Preliminary experiments were conducted using different  $\text{ZnSO}_4 \cdot 7\text{H}_2\text{O}\text{--NaOH}\text{--H}_3\text{BO}_3$  (ZSNaH) and  $\text{ZnCl}_2\text{--NaOH}\text{--H}_3\text{BO}_3$  (ZCNaH) molar ratios. ZSNaH and ZCNaH molar ratios of 1:2:6 [15] and 1:2:7 [16], respectively, were selected for further experiments.

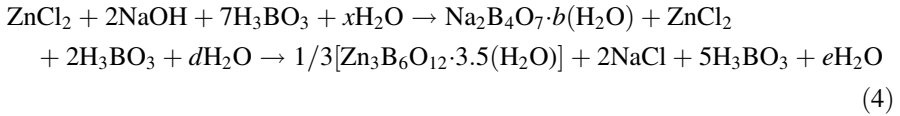
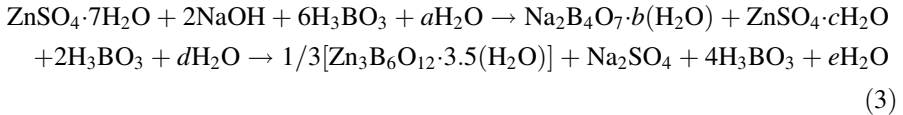
The reactions expected are shown in Eqs. (1) and (2):



To determine the effect of reaction temperature and reaction time on the product obtained, temperatures and reaction times were varied between  $70$  and  $90\ ^\circ\text{C}$  and from  $1\text{--}4\ \text{h}$ , respectively.

For experiments with ZSNaH,  $0.1329\ \text{mol}\ \text{H}_3\text{BO}_3$  was dissolved in  $25\ \text{ml}$  pure water obtained from GFL 2004 (Gesellschaft für Labortechnik, Burgwedel, Germany), then  $0.0210\ \text{mol}\ \text{ZnSO}_4 \cdot 7\text{H}_2\text{O}$  and  $0.0420\ \text{mol}\ \text{NaOH}$  were added to reactor. After addition of the raw materials, commercial zinc borate ( $\text{Zn}_3\text{B}_6\text{O}_{12} \cdot 3.5\ \text{H}_2\text{O}$ ), which was retrieved from a local market in Turkey ( $0.5\ \%$  w/w as  $\text{H}_3\text{BO}_3$ ) was added as seed agent for better crystallization. In ZCNaH experiments the amounts of  $\text{ZnCl}_2$  and NaOH were  $0.0190$  and  $0.0380\ \text{mol}$ , respectively.

pH changes in the reaction medium were recorded by use of a Hanna Instruments HI 2211 pH/ORP meter. The pure water had a pH of  $5.50 \pm 0.10$  (at  $24\ ^\circ\text{C}$ ). On addition of  $\text{H}_3\text{BO}_3$  the pH of the medium decreased to  $3.60 \pm 0.15$  (between  $70$  and  $90\ ^\circ\text{C}$ ). On addition of the zinc source the pH increased to  $3.70 \pm 0.02$  (between  $70$  and  $90\ ^\circ\text{C}$ ). On addition of NaOH the pH increased to  $5.85 \pm 0.20$  (between  $70$  and  $90\ ^\circ\text{C}$ ). Because the medium was acidic, semi-products of sodium borates were formed in the synthesis then the  $\text{Na}^+$  cation was exchanged with the  $\text{Zn}^{2+}$  cation and zinc borates were formed. The reaction scheme was, thus, as depicted in Eqs. (3) and (4):



The raw materials were reacted in a closed temperature-controlled vessel. After specific reaction times the solution was filtered through a Whatman blue ribbon filter paper and the crystallized products on the filter paper were washed three times with pure water (approximately 1,000 ml) at 50–60 °C, to remove unreacted reagents and Na<sub>2</sub>SO<sub>4</sub> and NaCl by-products, then dried in an incubator (Ecozell 111, Germany) at 105 °C for 24 h. The experimental method is shown schematically in Fig. 1.

### Characterization of zinc borate

Zinc borate was characterized by use of XRD, and FT-IR and Raman spectroscopy. For XRD, the conditions were the same as for characterization of the raw materials.

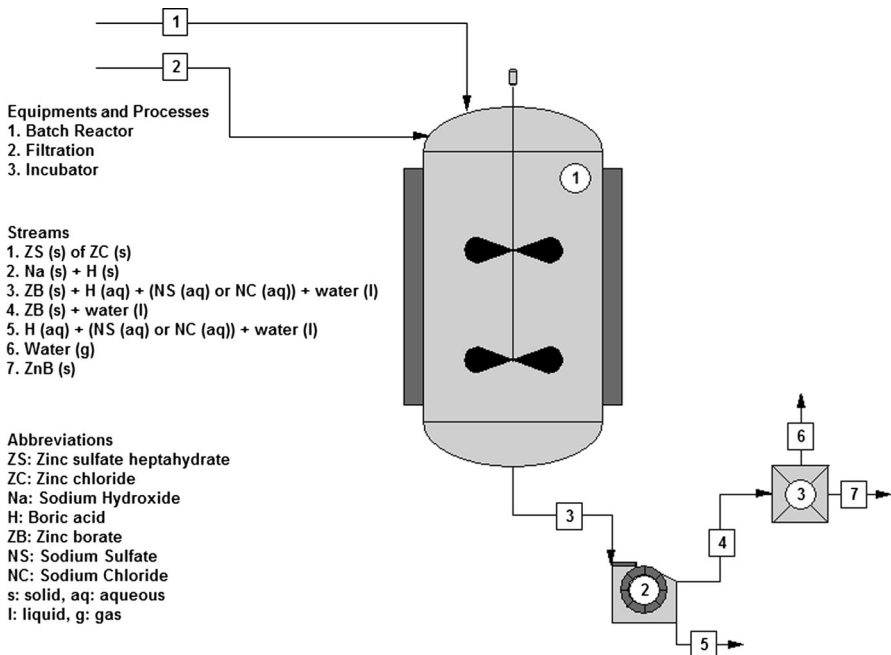


**Fig. 1** Schematic diagram of the experimental method

The range was between 10° and 70°, in accordance with literature reports of the location of the characteristic peaks of zinc borate hydrates.

The characteristic peaks of borate compounds are in the range 500–1,500 cm<sup>-1</sup> [17]; thus, the spectral ranges for FT-IR and Raman were set to 1,800–650 and 1,800–250 cm<sup>-1</sup>, respectively. No peak was observed above 1,800 cm<sup>-1</sup> in either FT-IR or Raman analysis.

Analysis of the surface morphology and particle size of the synthesized zinc borates was conducted by use of a CamScan Apollo 300 field-emission SEM (FESEM) at 15 kV. A backscattering electron detector (BEI) was used, and the magnification was set to 10.000.

Yield analysis was performed by use of the procedures of Derun et al. [18] and Kipcak et al. [19–22] with ZnSO<sub>4</sub>·7H<sub>2</sub>O and ZnCl<sub>2</sub> defined as the key components for ZSNaH and ZCNaH, respectively. Three identical experiments were performed and average yields were calculated.

To calculate the overall yield, *Y<sub>D</sub>*, the number of moles of the final product, *N<sub>D</sub>*, was divided by the number of moles of the key reactant, *A*, consumed. The number of moles of *A* consumed was calculated from the initial (*N<sub>A0</sub>*) and the final (*N<sub>A</sub>*) numbers of moles of reactant, by use of Eq. (5) [23].

$$Y_D = \frac{N_D}{N_{A0} - N_A} \tag{5}$$

### Thermal dehydration and kinetic study

The thermal properties of zinc borate samples were analyzed in the temperature range 105–620 °C with heating rates of 2, 5, 10, 15, 20 °C/min, under a nitrogen atmosphere, by use of Perkin Elmer Diamond DTA/TG. The kinetic data activation energy (*E<sub>a</sub>*) and exponential factor (*A<sub>o</sub>*) were calculated by use of the Coats–Redfern and Horowitz–Metzger methods.

In the Coats–Redfern non-isothermal kinetic method, a plot of ln[−ln(1 − α)] as a function of 1/*T* for *n* = 1.0 or a plot of ln[(1 − (1 − α)<sup>1−*n*</sup>)/(1 − *n*)] as a function of 1/*T* for *n* ≠ 1 gives the value of *E<sub>a</sub>* from the slope and the value of *A<sub>o</sub>* from the intercept.

$$\ln\left(-\frac{\ln(1 - \alpha)}{T^2}\right) = \ln\left(\frac{A_o R}{\beta E_a}\left(1 - \frac{2RT}{E_a}\right)\right) - \frac{E_a}{RT} \quad n = 1 \tag{6}$$

$$\ln\left(-\frac{(1 - (1 - \alpha)^{1-n})}{(1 - n)T^2}\right) = \ln\left(\frac{A_o R}{\beta E_a}\right) - \frac{E_a}{RT} \quad n \neq 1 \tag{7}$$

where α is the degree of dehydration or conversion, *R* is the gas constant, *n* is the order of the reaction, *T* is the absolute temperature, and β is the heating rate.

In the Horowitz–Metzger method, a plot of ln[−ln(1 − α)<sup>2</sup>] as a function of θ for *n* = 1.0 or a plot of ln[(1 − (1 − α)<sup>1−*n*</sup>)/(1 − *n*)<sup>2</sup>] as a function of θ for *n* ≠ 1

gives the value of  $E_a$  from the slope and value of  $A_0$  from the intercept.  $T_S$  is the peak of the DTG curve and  $\theta = T - T_S$ .

$$\ln(-\ln(1 - \alpha)) = \ln\left(\frac{A_0RT_s^2}{\beta E_a}\right) - \frac{E_a}{RT_s} + \frac{E_a\theta}{RT_s^2} \quad n = 1 \quad (8)$$

$$\ln\left(\frac{1 - (1 - \alpha)^{1-n}}{1 - n}\right) = \ln\left(\frac{A_0RT_s^2}{\beta E_a}\right) - \frac{E_a}{RT_s} - \frac{E_a\theta}{RT_s^2} \quad n \neq 1 \quad (9)$$

After the thermal analysis, zinc borate samples were heated in a Protherm MOS 180/4 high-temperature furnace set to increase at 10 °C/min to a temperature of 620 °C under a nitrogen atmosphere flowing at 5 ml/min. XRD analysis was then used to investigate the characteristics of the calcined zinc borate.

## Experimental results

### Results from characterization of the raw material

According to the XRD results obtained from the raw materials, the source of zinc,  $ZnSO_4 \cdot 7H_2O$ , was a mixture of two phases, bianchite ( $ZnSO_4 \cdot 6H_2O$ ), with the powder diffraction file (pdf) number 01-075-0949, and goslarite ( $ZnSO_4 \cdot 7H_2O$ ), with the pdf number 00-009-0395. Another source of zinc,  $ZnCl_2$ , was a mixture of two different forms of zinc chloride with powder diffraction file (pdf) numbers 01-074-0519 and 01-070-1284, respectively. The boron source,  $H_3BO_3$ , was determined to be sassolite ( $H_3BO_3$ ), pdf number 01-073-2158, and the boron and sodium source  $Na_2B_4O_7 \cdot 5H_2O$  was determined to be tincalconite ( $Na_2B_4O_7 \cdot 5H_2O$ ), pdf number 00-007-0277. The commercial zinc borate raw material was found to be zinc oxide borate hydrate ( $Zn_3B_6O_{12} \cdot 3.5H_2O$ ), pdf number 00-035-0433.

### XRD results for the synthesized zinc borates

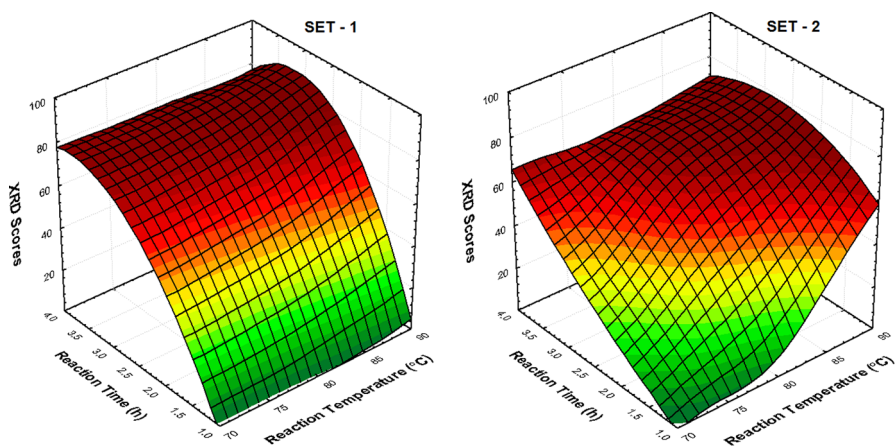
XRD scores for zinc borates synthesized at different temperatures for different reaction times are listed in Table 1. Synthesized zinc borate was found to be zinc oxide borate hydrate ( $Zn_3B_6O_{12} \cdot 3.5H_2O$ ), pdf number 00-035-0433. The different XRD scores for synthesized zinc borates in Set-1 and Set-2, as a result of different reaction time and temperature, are shown in Fig. 2. In Fig. 2, drawn by use of Statsoft Statistica software, the y-axis shows the XRD score (with a perfect crystal score set to 100), the z-axis shows the reaction temperature, and the x-axis shows the reaction time. The results from XRD indicate that with increasing time and temperature the XRD scores of the zinc borates increased.

In Set-1 experiments, zinc borate was prepared by use of a reaction temperature of 70 °C and reaction times of 3 and 4 h. The zinc borates obtained were coded in the format “set code-reaction temperature-reaction time”, where the set codes were “ZSNaH” for the set  $ZnSO_4 \cdot 7H_2O - NaOH - H_3BO_3$  and “ZCNaH” for the set

**Table 1** XRD scores of zinc borates synthesized from  $\text{ZnSO}_4 \cdot 7\text{H}_2\text{O}$ ,  $\text{ZnCl}_2$ ,  $\text{NaOH}$ , and  $\text{H}_3\text{BO}_3$ 

Temperature ( $^{\circ}\text{C}$ )	Time (h)	Set 1 (ZSNaH)	Set 2 (ZCNaH)
90	1	–	59 <sup>a</sup>
90	2	78	75
90	3	77	75
90	4	79	72
80	1	–	–
80	2	26 <sup>a</sup>	61
80	3	81	64
80	4	77	66
70	1	27 <sup>a</sup>	–
70	2	47 <sup>a</sup>	20 <sup>a</sup>
70	3	80	30 <sup>a</sup>
70	4	76	70

<sup>a</sup> Crystal formation was not complete

**Fig. 2** XRD formation graph for zinc borates synthesized by use of different reaction times and reaction temperatures

$\text{ZnCl}_2$ – $\text{NaOH}$ – $\text{H}_3\text{BO}_3$ . For example the product synthesized at  $70\text{ }^{\circ}\text{C}$  for 4 h by use of  $\text{ZnSO}_4 \cdot 7\text{H}_2\text{O}$ – $\text{NaOH}$ – $\text{H}_3\text{BO}_3$  was coded as “ZSNaH-70-4”. For reaction times of 1 and 2 h, some expected zinc borate peaks were seen but formation was not complete. In Set-2 experiments, amorphous product(s) were obtained after reaction for 1 h. After reaction for 2 and 3 h some expected zinc borate peaks were seen but formation was not complete. After reaction for 4 h formation of zinc borates was achieved. After reaction at  $80\text{ }^{\circ}\text{C}$  for 1 h an amorphous product was obtained and zinc borate formation was not complete in 2 h in Set-1 experiments. In contrast, in Set-2 experiments formation of zinc borate was successful after 2 h. After 3 h and 4 h in both sets of experiments zinc borate with high XRD scores was obtained. At  $90\text{ }^{\circ}\text{C}$  zinc borates were obtained after reaction for 2 h, after 1 h some zinc borate

peaks and amorphous products were observed in Set-2 and Set-1, respectively. Comparison of all the XRD results revealed that the products obtained from Set-1 had better crystal scores than those from Set-2.

XRD patterns of selected zinc borates are shown in Fig. 3. According to Fig. 3, the characteristic peaks and respective miller indexes ( $h k l$ ) and  $d$  spacing [ $\text{\AA}$ ] of synthesized zinc borates were determined as  $17.7^\circ$  ( $1\ 1\ -1$ ) ( $5.88\ \text{\AA}$ ),  $18.1^\circ$  ( $0\ 2\ 0$ ) ( $4.90\ \text{\AA}$ ),  $20.6^\circ$  ( $1\ 0\ 1$ ) ( $4.30\ \text{\AA}$ ),  $21.8^\circ$  ( $1\ 2\ 0$ ) ( $4.08\ \text{\AA}$ ),  $23.7^\circ$  ( $1\ 2\ -1$ ) ( $3.74\ \text{\AA}$ ),  $25.8^\circ$  ( $2\ 1\ 0$ ) ( $3.44\ \text{\AA}$ ),  $28.8^\circ$  ( $0\ 1\ 2$ ) ( $3.10\ \text{\AA}$ ),  $30.2^\circ$  ( $2\ 2\ 1$ ) ( $2.95\ \text{\AA}$ ), and  $36.8^\circ$  ( $2\ 3\ 0$ ) ( $2.44\ \text{\AA}$ ).

Results from FT-IR and Raman spectral analysis of the synthesized products

FT-IR and Raman spectra of the synthesized zinc borates were given in Figs. 4 and 5, respectively.

In FT-IR spectra (Fig. 4), asymmetrical and symmetrical stretching bands of three-coordinate boron to oxygen ( $\nu_{\text{as}}(\text{B}_{(3)}\text{-O})$ ) were observed in the ranges  $1,407\text{--}1,251$  and  $924\text{--}886\ \text{cm}^{-1}$ , respectively. The bands between  $1,067\text{--}980$  and  $856\text{--}855\ \text{cm}^{-1}$ , correspond to asymmetrical ( $\nu_{\text{as}}(\text{B}_{(4)}\text{-O})$ ) and symmetrical ( $\nu_{\text{s}}(\text{B}_{(4)}\text{-O})$ ) stretching, respectively, of four-coordinate boron to oxygen. Bands ascribed to bending of boron-

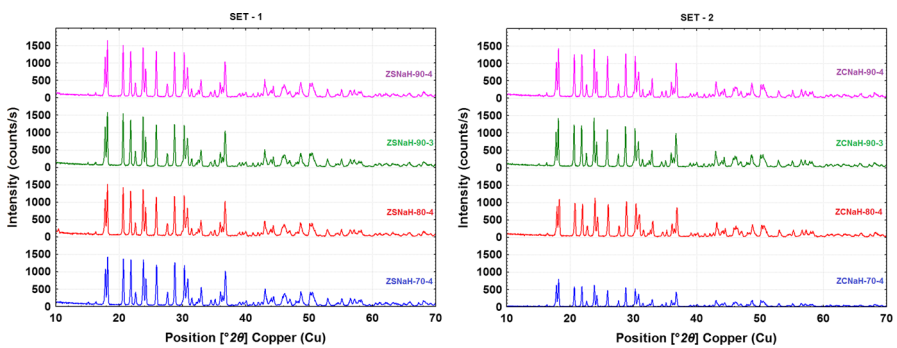


**Fig. 3** XRD patterns of synthesized zinc borates from Set-1 (ZSNaH) and Set-2 (ZCNaH)

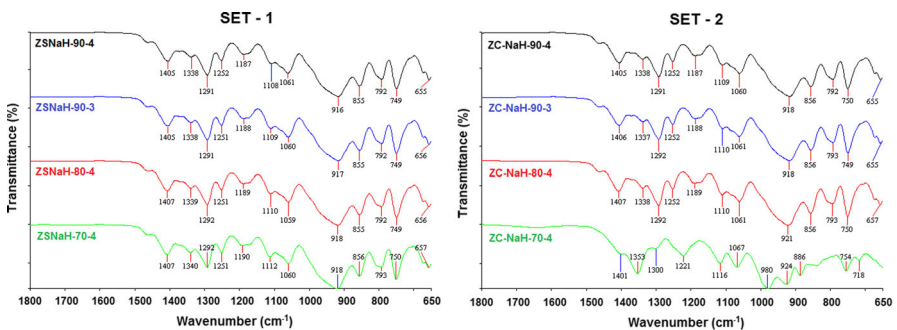


**Fig. 4** FT-IR spectra of the synthesized zinc borates from Set-1 (ZSNaH) and Set-2 (ZCNaH)



oxygen hydrogen bonds ( $\delta(\text{B}-\text{O}-\text{H})$ ) and bending of three-coordinate boron to oxygen ( $\gamma(\text{B}_{(3)}-\text{O})$ ) were seen between 1,221 and 1,108 and between 657 and 655  $\text{cm}^{-1}$ , respectively. The  $\nu_{\text{p}}(\text{B}(\text{OH})_4)^-$  band was in the range 793–718  $\text{cm}^{-1}$ .

In the Raman spectra (Fig. 5),  $\nu_{\text{as}}(\text{B}_{(3)}-\text{O})$  and  $\nu_{\text{s}}(\text{B}_{(3)}-\text{O})$  bands were seen in the ranges 1,294–1,292 and 920–919  $\text{cm}^{-1}$ , respectively. Bands between 1,049 and 1,037 and between 849 and 755  $\text{cm}^{-1}$  correspond to  $\nu_{\text{as}}(\text{B}_{(4)}-\text{O})$  and  $\nu_{\text{s}}(\text{B}_{(4)}-\text{O})$ , respectively.  $\delta(\text{B}-\text{O}-\text{H})$  and  $\gamma(\text{B}_{(3)}-\text{O})$  bands were seen between 1,190 and 1,187 and between 665 and 664  $\text{cm}^{-1}$ , respectively. The last two regions, which correspond to  $\delta(\text{B}_{(3)}-\text{O})/\delta(\text{B}_{(4)}-\text{O})$  and  $\delta(\text{B}_{(4)}-\text{O})$ , were between 596 and 578 and between 437 and 296  $\text{cm}^{-1}$ .

The results obtained from FT-IR and Raman spectroscopy were in good agreement with literature data [24, 25].

### Surface morphology and particle size of the synthesized zinc borates

The synthesized zinc borate hydrate specimens were subjected to SEM analysis to determine how reaction time and temperature affected the products. The surface morphology and particle size of zinc borate hydrates are shown in Fig. 6. Heterogeneous mixtures of round and rectangular crystals were obtained from Set-1 experiments performed at 70 °C. In contrast, thin cylindrical crystals were obtained from the Set-2 experiments. In both sets, proper particle formation was observed when reaction temperatures higher than 70 °C were used. Better rectangular crystals were obtained from Set-2 experiments than from Set-1 experiments. There were minor differences between the particle sizes obtained in each set. The best crystals were obtained by synthesis at 90 °C for 240 min in Set-2.

The particle sizes of the zinc borate hydrates obtained by use of different reaction conditions were on the micron scale for both sets. For the ZSNaH set, the shapes and particle sizes of the crystals were irregular at the lower temperatures. After reaction at 70 °C, crystal sizes ranged from 315 nm to 694 nm. After reaction at 80 °C, the minerals obtained had rectangle-like particle shapes and the crystal sizes ranged from 280 nm to 1.15  $\mu\text{m}$ . The particles synthesized at 90 °C had more uniform distributions and the crystal sizes ranged from 303 nm to 1.29  $\mu\text{m}$ .

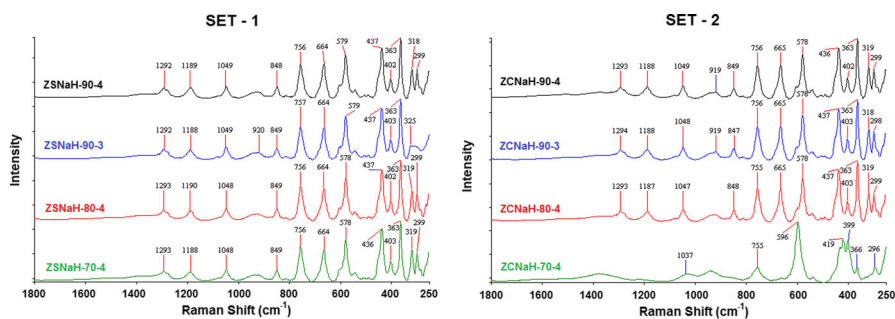


**Fig. 5** Raman spectra of the synthesized zinc borates from Set-1 (ZSNaH) and Set-2 (ZCNaH)

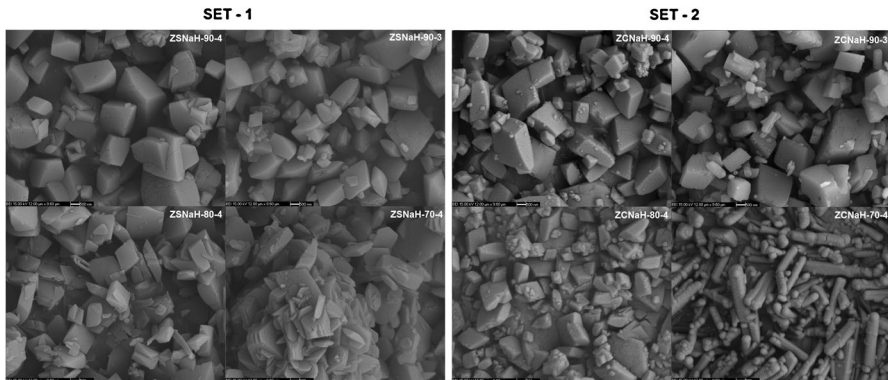


**Fig. 6** Morphology of synthesized zinc borates from Set-1 (ZSNaH) and Set-2 (ZCNaH) determined by SEM

In the ZCNaH set, temperature affected the morphology of synthesized compounds. At 70 °C, the particles formed as one dimensional micro-rods of length 1.40–3.08  $\mu\text{m}$  and width 346–445 nm. With increasing temperature, rectangle-like particles were obtained in the range of 387 nm–1.48  $\mu\text{m}$ . Proper crystal shape formation was observed after reaction at 90 °C, and particle sizes were between 336 nm and 2.06  $\mu\text{m}$ .

#### Calculation of the yield of synthesized zinc borate hydrates

Figure 7 shows the reaction yields of the synthesized zinc borate hydrates; reaction yields increased with increasing temperature and reaction times for both sets. In the set ZCNaH, higher reaction yields were observed at 90 °C and lower reaction yields were observed at 80 °C and 70 °C. Reaction yields were calculated to be between 88.1–96.7 and 76.5–98.9 % for the sets ZSNaH and ZCNaH, respectively.

Highest reaction yields were  $96.7 \pm 1.1$  and  $98.9 \pm 0.8$  % for the sets ZSNaH and ZCNaH, respectively.

#### Thermal analysis and dehydration kinetic results

TG and DTG analysis curves for pure synthesized  $\text{Zn}_3\text{B}_6\text{O}_{12} \cdot 3.5\text{H}_2\text{O}$  are shown in Fig. 8.

The curves show that  $\text{Zn}_3\text{B}_6\text{O}_{12} \cdot 3.5\text{H}_2\text{O}$  lost its water of crystallization in two steps, represented by two endothermic peaks. At a heating rate of 2 °C/min, in the first step of the dehydration process zinc borate hydrate lost 7.03 % of its weight in the range 261.61–391.86 °C. The peak temperature of DTG was at 382.72 °C. In the second step the initial, peak, and final temperatures were 391.86, 412.53, and 601.69 °C, respectively. The weight decrease in the second step was 6.37 %, for a total mass loss of 13.40 %. The initial, peak, and final temperatures on the TG and DTG curves and total weight losses are given in Table 2. In Table 2, the mass losses at each heating rate varied between 7.03 and 9.14 and between 4.78 and 6.38 % in the first and second steps, respectively.

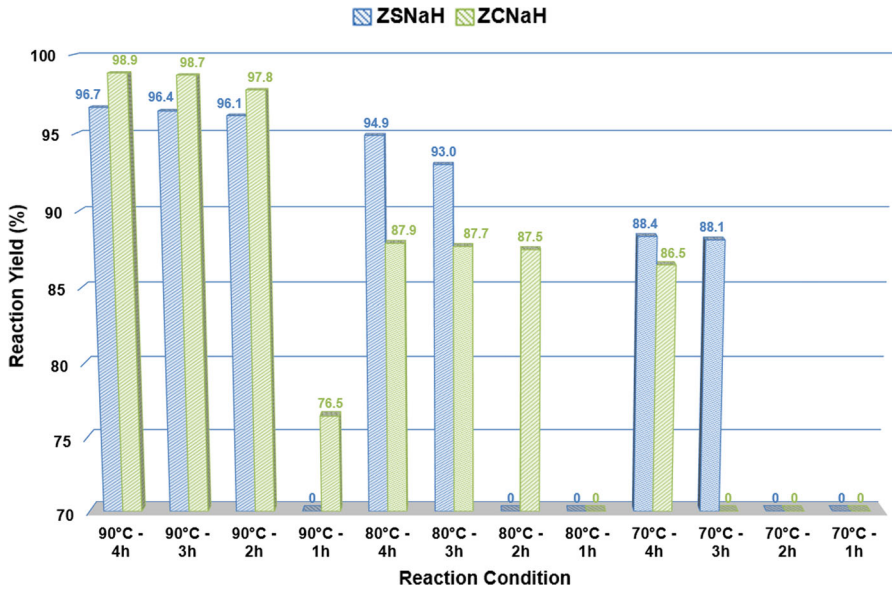
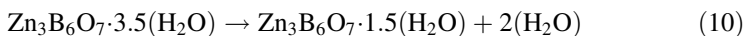


Fig. 7 Reaction yields of the synthesized zinc borates

The kinetic data  $E_a$  and  $A_0$  were calculated for conversion values ( $\alpha$ ) of 0.03–0.995 for the first step and 0.2–0.95 for the second step, by use of the Coats–Redfern and Horowitz–Metzger kinetic methods. Calculated values are given in Table 3. Correlation coefficients ( $R^2$ ) and the similarity of the results obtained show that these kinetic methods were suitable for study of the kinetics of dehydration of zinc borate.

Values of  $A_0$  obtained by use of the Coats–Redfern method were in the range  $1.03 \times 10^{17}$ – $4.09 \times 10^{18}$  for the first step of dehydration and  $7.43 \times 10^{36}$ – $8.61 \times 10^{53}$  for the second step.  $E_a$  values were determined as 225.40 and 570.63 kJ/mol for the first and second steps, respectively. Values of  $A_0$  obtained by use of the Horowitz–Metzger kinetic method were between  $1.67 \times 10^{19}$  and  $3.68 \times 10^{20}$  for the first step of dehydration and between  $3.17 \times 10^{37}$  and  $2.24 \times 10^{55}$  for the second step.  $E_a$  values were determined as 254.33 and 518.22 kJ/mol for the first and second steps, respectively. Because of the presence 3.5 mol water of crystallization in the structure of synthesized  $Zn_3B_6O_{12} \cdot 3.5H_2O$ , removal of water could be explained by a dehydration mechanism. In contrast with some types of boron mineral, the structure of  $Zn_3B_6O_{12} \cdot 3.5H_2O$  does not contain hydroxyl ions, so dehydroxylation was not observed.

The reaction schemes expected for the dehydration steps are given in Eqs. (10) and (11).



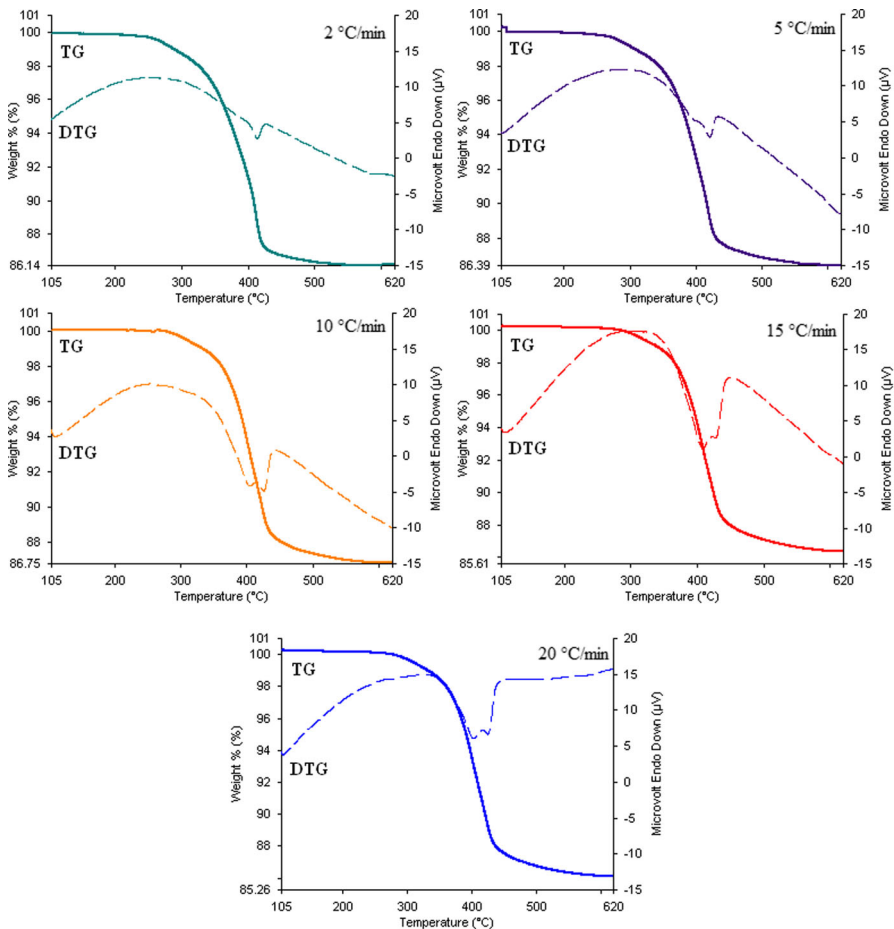
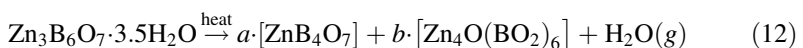


**Fig. 8** TG–DTG curves for  $\text{Zn}_3\text{B}_6\text{O}_{12}\cdot 3.5\text{H}_2\text{O}$

The thermal conversion results showed that calcined  $\text{Zn}_3\text{B}_6\text{O}_{12}\cdot 3.5\text{H}_2\text{O}$  lost approximately 13.6 % of its weight. This result, which is equal to 3.5 molar equivalents of water, was in accord with TG analysis. This indicates that the zinc borate hydrate lost all of its structural water and was transformed into a dehydrated zinc borate type of compound. The XRD result for calcined zinc borate hydrate revealed two different types of dehydrated zinc borate,  $\text{ZnB}_4\text{O}_7$  (pdf no 01-071-0634) and  $\text{Zn}_4\text{O}(\text{BO}_2)_6$  (pdf no 01-076-0917), were formed. The reaction scheme for the calcination is given in Eq. (12).



Crystallographic data for synthesized and calcined zinc borate hydrate are listed in Table 4. The XRD pattern of calcined zinc borate hydrate is shown in Fig. 9.

**Table 2** Results from thermal analysis of synthesized zinc borate ZSNaH-90-3

Heating rate (°/min)	Step	TG		DTG			$\Delta m$ (%)	Total $\Delta m$ (%)
		$T_i$ (°C)	$T_f$ (°C)	$T_i$ (°C)	$T_p$ (°C)	$T_f$ (°C)		
2	1	261.61	391.86	337.22	382.72	393.28	7.03	13.40
	2	391.86	601.69	393.28	412.53	427.97	6.37	
5	1	262.09	405.82	340.62	399.65	405.82	7.88	13.31
	2	405.82	606.24	405.82	419.55	440.83	5.43	
10	1	263.14	412.44	342.10	403.91	413.00	8.20	13.22
	2	412.44	608.94	413.00	421.56	452.11	5.02	
15	1	264.37	415.85	342.17	407.06	413.14	8.59	13.73
	2	415.85	609.86	413.14	421.70	452.35	5.14	
20	1	266.25	416.28	343.09	404.35	414.67	9.14	13.92
	2	416.28	610.22	414.67	422.41	453.55	4.78	

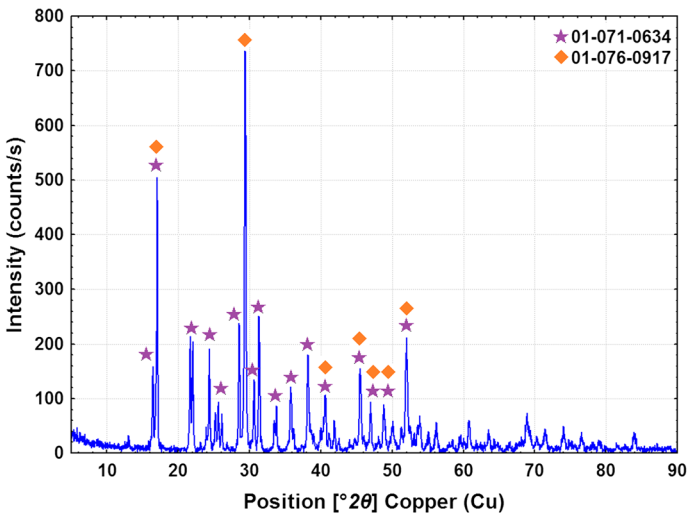
**Table 3** Data calculated by use of the kinetic methods

Heating rate (°/min)	Coats–Redfern method			Horowitz–Metzger method		
	$R^2$	Exponential factor ( $A_o$ )	Activation energy ( $E_a$ , kJ)	$R^2$	Exponential factor ( $A_o$ )	Activation energy ( $E_a$ , kJ)
<i>1st step</i>						
2	0.98	$4.09 \times 10^{18}$	242.12	0.98	$3.68 \times 10^{20}$	273.22
5	0.99	$1.20 \times 10^{17}$	223.06	0.99	$1.67 \times 10^{19}$	249.89
10	0.99	$1.03 \times 10^{17}$	220.95	0.99	$2.36 \times 10^{19}$	251.40
15	0.99	$1.64 \times 10^{17}$	221.59	0.99	$2.88 \times 10^{19}$	250.27
20	0.99	$1.42 \times 10^{17}$	219.27	0.99	$2.06 \times 10^{19}$	246.88
	Average activation energy		225.40	Average activation energy		254.33
<i>2nd step</i>						
2	0.98	$8.61 \times 10^{53}$	711.29	0.99	$2.24 \times 10^{55}$	716.09
5	0.99	$6.01 \times 10^{46}$	621.56	0.99	$6.02 \times 10^{47}$	616.35
10	0.98	$2.15 \times 10^{38}$	511.69	0.98	$1.00 \times 10^{38}$	491.09
15	0.98	$1.09 \times 10^{39}$	519.48	0.99	$1.27 \times 10^{38}$	490.69
20	0.98	$7.43 \times 10^{36}$	489.15	0.98	$3.17 \times 10^{37}$	474.73
	Average activation energy		570.63	Average activation energy		518.22

According to the Fig. 9, the five major characteristic peaks and their respective Miller indexes ( $h k l$ ) and  $d$  spacing (Å) of  $ZnB_4O_7$  and  $Zn_4O(BO_2)_6$  were determined as  $16.9^\circ$  (2 1 0) (5.23 Å),  $21.6^\circ$  (1 0 2) (4.12 Å),  $21.9^\circ$  (0 2 0) (4.06 Å),  $28.4^\circ$  (3 0 2) (3.14 Å),  $31.3^\circ$  (3 2 1) (2.86 Å) and  $29.2^\circ$  (2 1 1) (3.05 Å),  $38.0^\circ$  (3 1 0) (2.36 Å),  $45.3^\circ$  (3 2 1) (2.00 Å),  $48.7^\circ$  (4 0 0) (1.87 Å),  $51.8^\circ$  (3 3 0) (1.76 Å), respectively.

**Table 4** Crystallographic data for synthesized and calcined zinc borate hydrates

Mineral	Zinc oxide borate hydrate	Zinc borate	Zinc borate
Pdf no.	00-035-0433	01-071-0634	01-076-0917
Chemical formula	$Zn_3B_6O_{12} \cdot 3.5H_2O$	$ZnB_4O_7$	$Zn_4O(BO_2)_6$
Molecular weight (g/mol)	516.08	220.63	534.42
Crystal system	Monoclinic	Orthorhombic	Cubic
Space group	P21/n (no: 14)	Pbca (no:61)	I-43 m (no: 217)
$a$ (Å)	7.6950	13.7140	7.4800
$b$ (Å)	9.8028	8.0910	7.4800
$c$ (Å)	6.8378	8.6310	7.4800
$\alpha$ (°)	90.00	90.00	90.00
$\beta$ (°)	107.03	90.00	90.00
$\gamma$ (°)	90.11	90.00	90.00
$z$	2.00	8.00	2.00
Density (calculated) ( $g\ cm^{-3}$ )	2.93	3.06	4.24

**Fig. 9** XRD pattern of calcined zinc borate hydrate

## Conclusions

In this study a  $Zn_3B_6O_{12} \cdot 3.5H_2O$ -type zinc borate was synthesized under moderate reaction conditions with very high yield from the starting zinc sources  $ZnSO_4 \cdot 7H_2O$  and  $ZnCl_2$ . XRD results showed that the zinc borates could be synthesized by reaction at 70 °C for 4 h, at 80 °C for 3 h, and at 90 °C for 2 h. The highest yields were obtained by reaction at 90 °C for 4 h for both ZSNaH and ZCNaH, with yields of 96.7 and 98.9 %, respectively. SEM results showed that homogeneous products were obtained at the highest temperatures. Thermal studies showed that

$Zn_3B_6O_{12} \cdot 3.5H_2O$  lost its water of crystallization in two steps, forming the dehydrated zinc borate compounds  $ZnB_4O_7$  and  $Zn_4O(BO_2)_6$ . Kinetic studies were conducted by use of the Coats–Redfern and Horowitz–Metzger methods; average activation energies were in the ranges 225.40–254.33 and 570.63–518.22 kJ/mol, for the first and second steps, respectively.

## References

1. D.M. Schubert, F. Alam, M.Z. Visi, C.B. Knobler, *Chem. Mater.* (2003). doi:10.1021/cm020791z
2. K.K. Shen, D.J. Ferm, *Boron Compounds as Fire Retardants, Flame Retardants—101: Basic Dynamics.* (Fire Retardant Chemicals Association, Pennsylvania, 1996), p.139
3. Y. Tian, Y. Guo, M. Jiang, Y. Sheng, B. Hari, G. Zhang, Y. Jiang, B. Zhou, Y. Zhu, Z. Wang, *Mater. Lett.* (2006). doi:10.1016/j.matlet.2006.01.108
4. X. Shi, Y. Xiao, M. Li, L. Yuan, J. Sun, *Powder Technol.* (2008). doi:10.1016/j.powtec.2007.12.014
5. M. Kilinc, G.O. Cakal, S. Yesil, G. Bayram, I. Eroglu, S. Ozkar, *J. Cryst. Growth* (2010). doi:10.1016/j.jcrysgro.2010.05.048
6. Y.H. Gao, Z.H. Liu, *Thermochim. Acta* (2009). doi:10.1016/j.tca.2008.11.013
7. Y. Tian, Y. He, L. Yu, Y. Deng, Y. Zheng, F. Sun, Zh Liu, Z. Wang, *Colloid Surf. A* (2008). doi:10.1016/j.colsurfa.2007.06.029
8. C. Ting, D.J. Cheng, W.L. Shuo, F. Gang, *J Mater Process Technol.* (2009). doi:10.1016/j.jmatprotec.2008.09.029
9. Y. Zheng, Y. Tian, H. Ma, Y. Qu, Z. Wang, D. An, S. Guan, X. Gao, *Colloid Surf. A* (2009). doi:10.1016/j.colsurfa.2009.02.018
10. N. Tugrul, M. Bardakci, E. Ozturk, *Res. Chem. Intermed.* (2014). doi:10.1007/s11164-014-1538-4
11. A.K. Galwey, *Thermochim. Acta* (2000). doi:10.1016/S0040-6031(00)00448-2
12. E.M. Derun, F.T. Senberber, *Sci. World J.* (2014). doi:10.1155/2014/985185
13. M. Gonen, D. Balkose, S. Ulku, J. Supercrit. Fluids (2011). doi:10.1016/j.supflu.2011.08.004
14. M. Gonen, D. Balkose, R.M. Gupta, S. Ulku, *Ind. Eng. Chem. Res.* (2009). doi:10.1021/ie9003046
15. N. Tugrul, A.S. Kipcak, E.M. Derun, S. Piskin, *Int. J. Chem. Nucl. Metall. Mater. Eng.* **8**, 7 (2014)
16. M. Piskin, A.S. Kipcak, M. Yildirim, T. Senberber, N. Tugrul, E.M. Derun, S. Piskin, Zinc chloride, sodium hydroxide and boric acid molar ratio determination for the production of zinc borates. TMS 2015 Annual Meeting & Exhibition, Orlando, FL, USA., 15–19 March 2015
17. A. Chen, P. Gu, S. Xu, Z. Ni, *Adv Mater Res* **399**, 343 (2012)
18. E.M. Derun, A.S. Kipcak, F.T. Senberber, M.S. Yilmaz, S. Piskin, *Res. Chem. Intermed.* (2013). doi:10.1007/s11164-013-1237-6
19. A.S. Kipcak, E.M. Derun, S. Piskin, *J. Chem.* (2013). doi:10.1155/2013/329238
20. A.S. Kipcak, D.Y. Baysoy, E.M. Derun, S. Piskin, *Adv. Mater. Sci. Eng.* (2013). doi:10.1155/2013/747383
21. A.S. Kipcak, E.M. Derun, S. Piskin, *Turk. J. Chem.* (2014). doi:10.3906/kim-1307-61
22. A.S. Kipcak, M. Yildirim, S.A. Yuksel, E.M. Derun, S. Piskin, *Adv. Mater. Sci. Eng.* (2014). doi:10.1155/2014/819745
23. H.S. Fogler, *Element of Chemical Reaction Engineering* (Prentice-Hall Press, New Jersey, 1999)
24. J. Yongzhong, G. Shiyang, X. Shuping, L. Lun, *Spectrochim. Acta Part A* (2000). doi:10.1016/S1386-1425(99)00227-9
25. R.L. Frost, *J. Raman Spectrosc.* (2010). doi:10.1002/jrs.2745